Lumbar Facet Joint Kinematics and Load Effects During Dynamic Lifting

Suman K. Chowdhury, Texas A&M University, College Station, USA, **Ryan M. Byrne**, University of Pittsburgh, Pennsylvania, USA, and **Yu Zhou** and **Xudong Zhang**, Texas A&M University, College Station, USA

Objective: To examine the lumbar facet joint kinematics in vivo during dynamic lifting and the effects of the load lifted.

Background: Although extensive efforts have been dedicated to investigating the risk factors of low back pain (LBP) associated with load handling in the workplace, the biomechanics of lumbar facet joints during such activities is not well understood.

Method: Fourteen healthy participants performed a load-lifting task while a dynamic stereo-radiography system captured their lumbar motion continuously. Data from 11 participants were included for subsequent analysis. A randomized block design was employed to study the load effect (4.5 kg, 9.0 kg, and 13.5 kg) on bilateral facet joint motions at approximately 60°, 40°, 20°, and 0° trunk-flexion postures. The facet orientations were also examined.

Results: Significant load effects were found for the flexion and lateral bending and superior-inferior translation of the facet joints. The L5-S1 displayed greater lateral bending and twisting, which was due to its more posterolateral orientation than the L2-L3, L3-L4, and L4-L5 facet joints. The left-right asymmetry in facet orientation was observed, most prominently at L3-L4 and L5-S1 facet joints.

Conclusion: The lumbar facet joint kinematics are affected by the magnitude of the lifted load and are dependent on the orientations of articulating adjacent facets.

Application: This study provided new insights into the role of lumbar facet joints in vivo during lifting. Alterations in the facet joint kinematics due to vigorous functional demand can be one of the primary but overlooked mechanical factors in the causation of LBP.

Keywords: low back pain, facet orientation, lumbar spine, trunk flexion, dynamic stereo X-ray system.

Address correspondence to Xudong Zhang, Department of Industrial & Systems Engineering, Texas A&M University, College Station, TX 77843, USA; e-mail: xudongzhang@tamu.edu.

HUMAN FACTORS
Vol. 60, No. 8, December 2018, pp. 1130–1145
DOI: 10.1177/0018720818790719

INTRODUCTION

Low back pain (LBP) continues to prevail as one of the most common and costliest musculoskeletal health problems experienced in the modern workplace. According to the Bureau of Labor Statistics (BLS), musculoskeletal disorders (MSDs) comprised approximately 31% of all work-related injuries in the United States in 2015, with low-back-related injuries making up 40% of all MSDs (BLS, 2016). According to a *Journal of Bone & Joint Surgery* study, the cumulative annual costs of LBP exceed $100 billion in the United States, two-thirds of which are indirect costs due to lost wages and reduced productivity (Katz, 2006).

To date, biomechanical studies have established the contribution of mechanical factors, including work intensity, static work postures, bending and twisting, lifting, pushing or pulling, and repetition to the risks of low back disorders in the workplace (Hoogendoorn, van Poppel, Bongers, Koes, & Bouter, 1999; Marras et al., 1995). Among these risk factors, both epidemiologic and biomechanical studies have documented that forceful exertion in the workplace, specifically lifting, predominantly contributes to the risk of LBP (Bigos et al., 1986; Hoogendoorn et al., 2000; Marras, Ferguson, Burr, Davis, & Gupta, 2004).

The increasing functional demands due to workplace risk factors have been substantially studied for low back structures such as muscles, vertebrae, and intervertebral discs (Granata & Marras, 1993; Marras & Sommerich, 1991; McGill & Norman, 1986; Zhang, Xiong, & Bishop, 2003). A comprehensive understanding of the functional demand in the low back requires investigating the effects of these risk factors on another principle support structure—the facet joints that preserve spinal stability by constraining motion between adjacent vertebrae (Adams & Hutton, 1981). However, the majority of the

previous studies have largely ignored the evaluation of facet joints under the influence of workplace risk factors.

Studies on the prevalence of LBP have recognized the lumbar facet joints as an important "piece of the puzzle" in the etiology of LBP (DePalma, Ketchum, & Saullo, 2011; Manchikanti et al., 2001). In general, facet joints play a crucial role in maintaining the spinal stability, and any deviation from their normal mechanics can adversely affect the integrity of an entire segment (Crawford et al., 2002). Facet injuries, such as unilateral or bilateral fractures or dislocations, can not only cause damage to the hard and soft tissues of the facet joint but also instigate injuries inflicted upon other soft tissues and structures in the spine, such as intervertebral discs and the spinal cord (Igarashi, Kikuchi, Konno, & Olmarker, 2004; Vaccaro et al., 1999).

A review of the literature exhibited numerous in vitro studies, animal models, and finite element simulations that primarily aimed to determine the mechanical function of the facet joints when various loads were applied to lumbar spines (Naserkhaki, Jaremko, Adeeb, & El-Rich, 2016; Otsuka et al., 2010; Panjabi et al., 1993; Popovich et al., 2013; Sharma, Langrana, & Rodriguez, 1995). A comprehensive literature search only identified one study by Kozanek et al. (2009), which reported in vivo kinematics of the lumbar facet joint in different trunk postures: maximal forward-backward bend, side-to-side bending, and maximal left-right torsion. The lumbar spine was imaged using a dual-fluoroscopic imaging system when the participants held varied static torso positions for about 2 s.

Furthermore, studies have reported segmental variations in facet joint orientation in providing stability to the spine and controlling its motion under complex loading (Liu et al., 2017; Masharawi et al., 2004; Masharawi et al., 2005; Noren, Trafimow, Andersson, & Huckman, 1991; Panjabi et al., 1993). Some other studies have focused on the left-right distinction in facet orientation, i.e., facet tropism, which arguably may increase the risk of degererative diseases, such as disc herniation and rotational spinal instability (Grobler, Robertson, Novotny, & Pope, 1993; Grogan, Nowicki, Schmidt, & Haughton, 1997; Masharawi et al., 2005; Noren et al., 1991; Sharma et al., 1995). These studies however were either cadaver-based in vitro experiments or finite element analyses for nonfunctional body poses. Therefore, the influence of articular facet orientation on facet joint kinematics in vivo under functional loading remains a formidable research gap. In order to reduce or circumvent the risks of facet-related pathologies, such as facet degeneration, disc degeneration, and neural impingement, it is important to identify the work activities that incur abnormal or excessive facet joint motions.

Therefore, this article reports a study of the lumbar facet kinematics during a dynamic load-lifting task. A clear and quantitative understanding of the facet joint structure and motion and how they are affected by mechanical loading can provide much-needed insights into the role of the lumbar facet joints in occupational LBP. Given that the combined effect of torso flexion and external load is the foremost risk factor for LBP, we postulated that the magnitude of the load lifted would significantly affect the lumbar facet kinematics during a dynamic lifting task.

METHODS

Overview

Participants performed dynamic lifting of three different loads of 4.5 kg, 9 kg, and 13.5 kg from a trunk-flexed (~ 75º flexion) position to a final upright (~ 0º flexion) position within 2 s, while a dynamic stereo-radiography (DSX) system imaged their lumbar region continuously. The instantaneous, three-dimensional vertebral positions and orientations of the lumbar spine were determined from the dynamic X-ray and computed tomography (CT) images through a volumetric model-based tracking process. The six-degrees-of-freedom kinematics of the facet joints were determined by first defining a local coordinate system (LCS) on each facet surface and then estimating the body-fixed rotations and translations that quantified the difference in orientation between the two LCS of adjacent facet surfaces.

Participants

Fourteen young, healthy individuals (8 males—age: 24 ± 2 years; weight: 78 ± 9 kg;

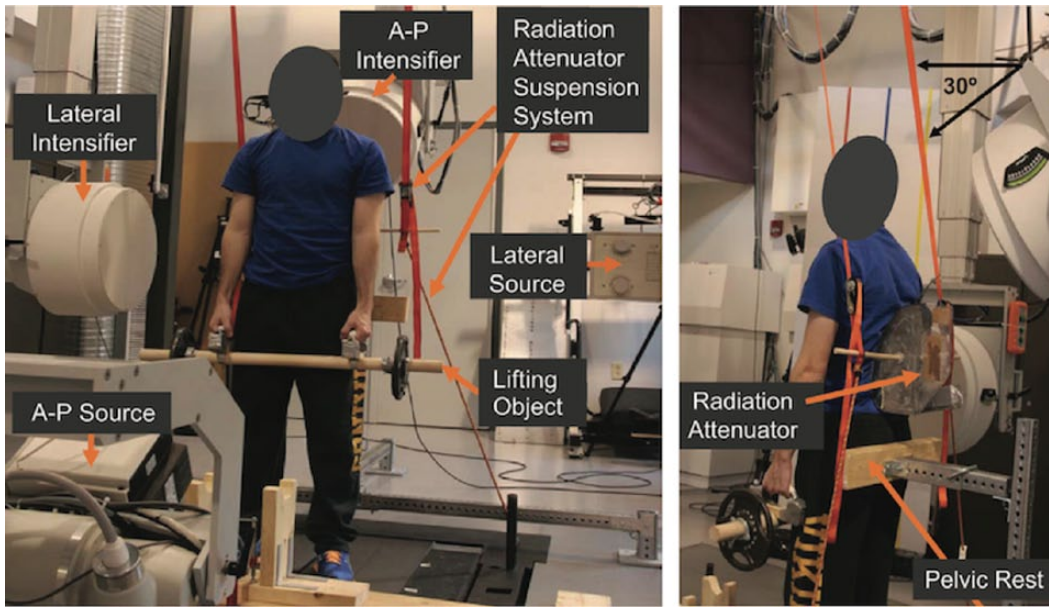

Figure 1. A dynamic stereo-radiography (DSX) system configured with custom-built add-on apparatus including a pelvic rest and a radiation attenuator to enable in vivo imaging of the lumbar spine region during the lifting task (Aiyangar et al., 2014).

height: 178 ± 7 cm, and 6 females—age: 25 ± 2 years; weight: 61 ± 8 kg; height: 170 ± 6 cm) with no prior history of any spinal disorder, injury, or notable pain were recruited from the local community to participate in this study. Out of these 14 participants, data from three participants (2 males and 1 female) were excluded due to poor image capture quality. Thus, data from 11 participants (6 males—age: 24.2 ± 1.9 years; weight: 75.7 ± 7.8 kg; height: 176.8 ± 7.4 cm, and 5 females—age: 25.5 ± 0.6 years; weight: 62.3 ± 8.5 kg; height: 170.3 ± 7.2 cm) were used for subsequent analysis and hypothesis-testing. All participants provided a signed consent form approved by the institutional review board.

Experimental Setup

Details of the experimental setup as shown in Figure 1 have been reported in prior publications (Aiyangar, Zheng, Anderst, & Zhang, 2015; Aiyangar, Zheng, Tashman, Anderst, & Zhang, 2014). Briefly, the *lifting object* comprised a radiolucent wooden dowel rod, weights, and two handles. The weights were symmetrically loaded on both sides of the rod, and the handles were affixed to the dowel rod approximately shoulder width apart. The *radiation attenuator* was devised to minimize the radiation white-out effects on the images and the *pelvic rest* to limit excessive pelvic anterior-posterior motion while participants performed the lifting task. The *DSX system* consists of two cardiac-cine angiography generators (EMD Technologies), two X-ray tubes with a 0.3/0.6 mm focal spot, two 16-in. Thalus image intensifiers, and two high-speed digital video cameras (4-megapixels Phantom v10, Vision Research). In this study, two X-ray tubes along with the high-speed cameras and image intensifiers were positioned in participants' mediolateral and anteroposterior directions such that their corresponding X-ray beams intersect at the lumbar region of the participants. The X-rays were generated at a rate of 30 frames per second with a pulsed exposure time of 4 ms/frame. The biplane X-ray images that were synchronically captured by the high-speed cameras were mapped to dimensions of 1800 × 1824 pixels (pixel size ~0.22 mm) and then down-sampled to 512 × 512 pixel resolution (~0.8 × 0.8 mm^2 pixel size). High-resolution CT

images of the lumbar spine were acquired using a CT scanner (LightSpeed Pro16, GE Medical Systems, Waukesha, WI).

Experimental Design

We employed a randomized complete block design (RCBD) to identify significant changes in the dependent variable as a function of the independent variable. The independent variables were the fixed effect of load with three levels—4.5 kg, 9 kg, and 13.5 kg and the randomized blocking variable—the effect of subjects. The dependent variables were the kinematics of L2-L3, L3-L4, L4-L5, and L5-S1 bilateral facet joints at four different time instances—0.5 s, 1 s, 1.5 s, and 2 s that corresponded to trunk-flexion angles at approximately 60º, 40º, 20º, and 0º, respectively. The RCBD (i.e., two-way ANOVA) was used to assess the load effect on the facet joint motions at each time instance (or posture).

Experimental Procedure

Participants performed the lifting task with a flexed torso (~75º) to a final upright trunk position in the midsagittal plane. The lifting object was initially placed in front of the participant at an approximate height of 35 cm from the floor, and the horizontal distance was adjusted to achieve an approximate torso flexion of 75°. A goniometer was used to determine the hip angle between the surface markers placed at the shoulder and knee of each participant in order to keep the initial trunk-flexed (~75º) position. The pelvic motions were restrained by instructing the participant to maintain light but constant contact between their pelvis and the pelvic rest, which also facilitated keeping the lifting task sagittally symmetric. Prior to the experiment, the participants underwent a few mock trials to ensure that they completed a trial within 2 s without knee bending. A metronome was used as a guide to ensure that the participants performed a trial within 2 s at a continuous, steady pace. Two trials (repetitions) were conducted at each load level, resulting in a total of six trials. Sufficient rest was provided between the trials such that the participants indicated readiness to continue and showed no sign of fatigue or discomfort. Upon completion of the laboratory experiment, CT scans of the lumbar region for each participant were acquired in a clinical facility with the following specifications: slice spacing of 1.25 mm, 12.8 cm field of view, and 512 × 512 pixels per image (0.547 mm/pixel in-plane resolution).

Data Processing

Model-based tracking. The instantaneous 3D vertebral bone positions were determined through a volumetric model-based tracking process, with submillimeter accuracy (precision ≤ 0.26º, 0.2 mm) as shown by a previous validation study (Lee & Anderst, 2010). The process required creating 3D vertebral bone models from the participants' CT scans using Mimics 14.0 (Materialise Inc., Ann Arbor, MI) and then placing the models in a virtual testing configuration that is identical to the DSX experimental setup (Figure 2).

The CT volume, defined as the outer cortical bone surface plus all interior bone tissue, was interpolated to create cubic voxels (0.25 mm × 0.25 mm × 0.25 mm). Given the DSX system and the 3D bone model, a pair of digitally reconstructed radiographs (DRRs) were generated via a volumetric ray-tracing algorithm (Figure 2). By maximizing the correlation between DRRs and the biplane radiographic images, the 3D position and orientation of the vertebrae were ascertained. This process was repeated for each vertebra across all frames of data.

Kinematic analysis. The facet joint kinematics were estimated for the complete cycle of motion of each trial by defining LCS on the individual facet surfaces of four lumbar and one sacral spine segments (L2-L5 and S1). Four consistently identifiable landmark points were placed on each facet surface (Figure 3a). The origin of the coordinate system was defined at the centroid of those four landmark points. The Z-axis was defined as the vector connecting the posterior-most landmark to the anterior-most landmark. A temporary axis was defined as the vector connecting the inferior-most landmark to the superior-most landmark. The X-axis was defined as the cross product of temporary axis and Z-axis. The Y-axis was then defined as the cross product of Z-axis and X-axis to create a right-handed Cartesian coordinate system. The

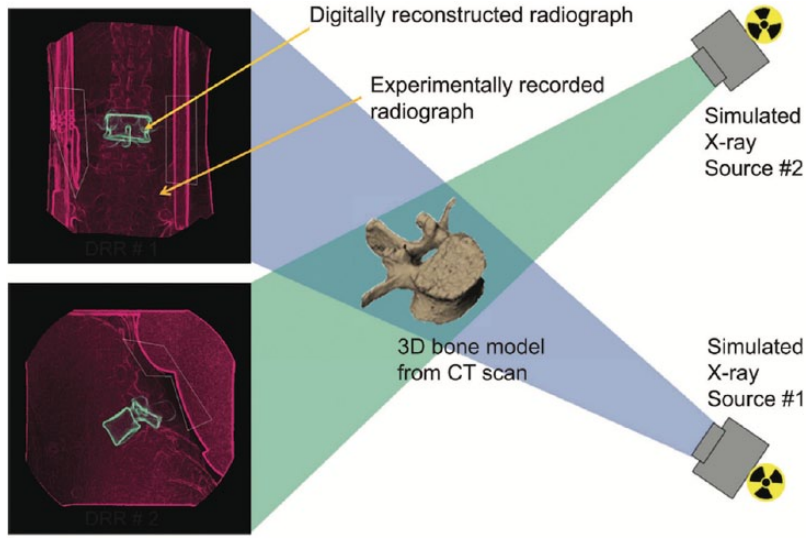

Figure 2. Graphical representation of the virtual testing configuration for the volumetric model-based bone tracking procedure.

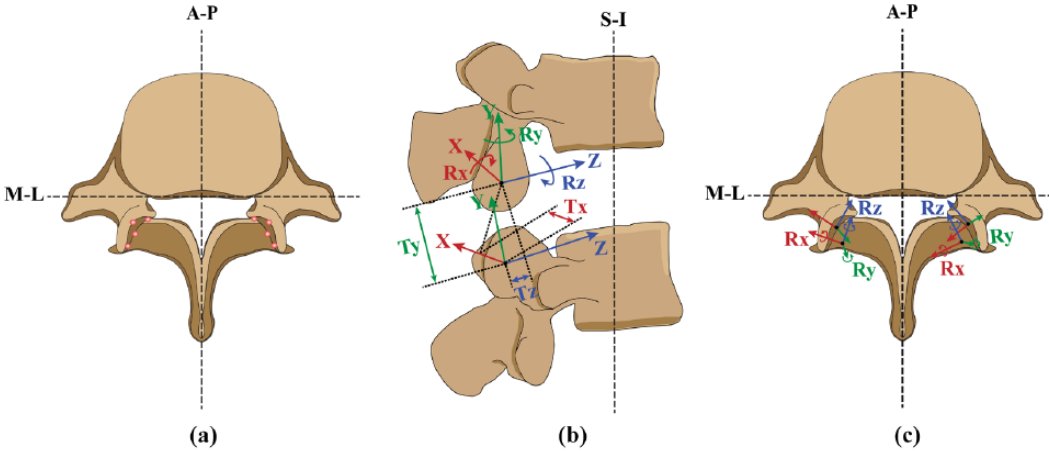

Figure 3. Measurements of facet joint kinematics: (a) placement of four landmarks at anterior-most, posterior-most, inferior-most and superior-most locations in each facet surface; (b) local coordinate system (LCS) established on the facet surfaces of two adjacent vertebras to define facet joint kinematics—flexion-extension (Rx), twisting (Ry), and lateral bending (Rz) motions, and medial-lateral (Tx), superior-inferior (Ty), and anterior-posterior (Tz) translations; and (c) left-side LCS created as the mirror image of the right-side LCS. The dotted lines—A-P, M-L, and S-I denote anterior-posterior, medial-lateral, and superior-inferior directions, respectively.

bilateral (left and right sides) facet-joint kinematics (three rotations: flexion-extension, lateral bending and twisting; and three translations: medial-lateral, anterior-posterior, and superior-inferior) were determined by body-fixed rotations of the lower facet of the superior vertebrae with respect to the upper facet of the inferior vertebrae using Euler principle (Figure 3b). We multiplied twisting and lateral bending motions and medial-lateral translation of the left facet by negative one—effectively creating a left-handed Cartesian coordinate system at the left facet—so that

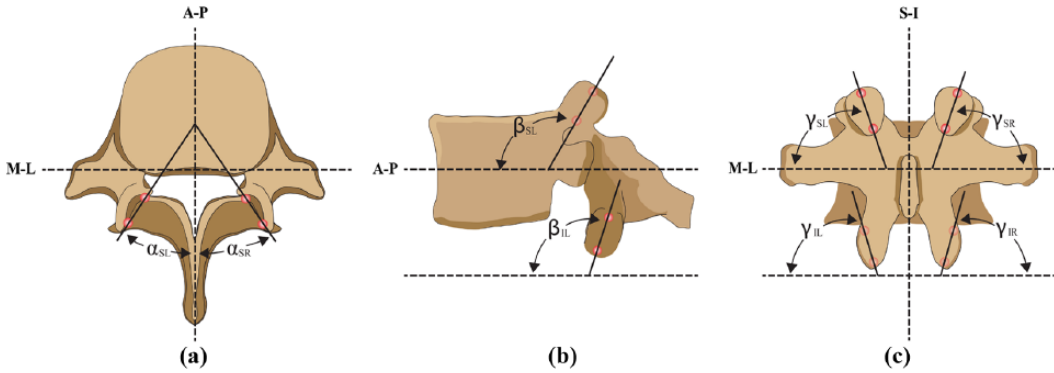

Figure 4. Measurements of facet surface orientation: (a) transverse facet angle (α), (b) sagittal facet angle (β), and (c) coronal facet angle (γ). The symbols—α_{SL} and α_{SR}, β_{SL} and β_{IL}, and γ_{SL}, γ_{SR}, γ_{IL}, and γ_{IR} respectively denote left and right transverse facet angles, superior and inferior left sagittal facet angles, and left-superior, right-superior, left-inferior, and right-inferior coronal facet angles. The symbols—A-P and M-L denote anterior-posterior and medial-lateral directions, respectively.

positive rotations at the left and right facet joints were symmetric about the sagittal plane (Figure 3c). The facet joint kinematics were estimated for the complete cycle of a trial for L2-L3, L3-L4, L4-L5, and L5-S1 facet joints. In this study, the L1-L2 facet joint motions could not be determined since L1 vertebrae went outside the capture volume of the DSX system during at least part of the cycle for most of the participants. Likewise, a few frames in the starting position (~ 75° trunk flexion) were not trackable owing to poor image quality. Thus, the starting time instance (t = 0 s) was not considered. The load effect was examined at four different time instances: t = 0.5 s, 1 s, 1.5 s, and 2 s. At each time instance, the kinematic data of each facet joint were calculated by averaging the data of three consecutive frames (Equation 1).

$$\bar{X}_t = \frac{X_{f-1} + X_f + X_{f+1}}{3} \qquad (1)$$

where t is the time instance, f is the frame number corresponding to t, and $\bar{X}_t$ is the average facet joint kinematic data at time t.

The time instances of 0.5 s, 1 s, 1.5 s, and 2 s corresponded to the trunk flexions of 56~60º, 36~40º, 17~20º, and −2~2º, respectively. To describe the load effect at those four time instances in a more coherent manner, these postural ranges, 56~60º, 36~40º, 17~20º, and −2~2º were rounded to their nearest tenth which would give values of 60º, 40º, 20º, and 0º, respectively.

Facet surface orientation. In this study, angular alignment of the articulating facet surface with respect to the transverse and sagittal planes of the spine defined the sagittal and vertical facet orientations, respectively. The transverse facet angle (α) was measured as the angle between the Z-axis of facet surface projected onto the transverse plane of the vertebrae and the anteroposterior axis lying in the midsagittal plane, indicating the coronal orientation of the facet geometry (Figure 4a). The sagittal facet angle (β) was the angle between the longitudinal axis—created by connecting the inferior- and superior-most markers along the facet length—projected onto the sagittal plane and the anteroposterior axis parallel to the transverse plane, implying both vertical and anteroposterior orientations of the facet geometry (Figure 4b). The coronal facet angle (γ) was the angle between the longitudinal axis—created by connecting the inferior- and superior-most markers along the facet length—projected onto the coronal plane and the mediolateral axis parallel to the transverse plane, entailing both vertical and mediolateral orientations of the facet geometry (Figure 4c).

Statistical Analysis

Descriptive statistics (such as mean and standard deviation) of the transverse, sagittal, and coronal facet angles were obtained across

all 11 participants. The kinematic data of two trials of each lifting load were averaged to perform the statistical analysis. The assumptions of the analysis of variance (ANOVA)—such as normality of residuals, homogeneity of variance residuals, and so forth—were first tested before conducting any ANOVA procedure. We performed 48 (4 time instances × 6 kinematic variables × 2 sides) two-way ANOVA procedures at each facet joint to observe the significant differences in the facet joint motion due to the effect of external load. These were further followed by the Fisher's least square differences when the main effect was found in a two-way ANOVA procedure to identify the differences in load magnitudes. Partial eta squared (η^2) was also estimated for the reference of the effect size. The partial η^2 values of 0.01~0.059, 0.06~0.139, and >0.14 were considered as small, medium, and large effect sizes, respectively (Cohen, 1988). Student's *t* tests were employed to evaluate left-right distinction in facet joint motions at each time instance.

Since the facet orientation data did not follow normal distribution, the Friedman test—a nonparametric statistical test—was chosen to examine the facet tropism: a left-right distinction in facet joint orientation. A p-value ≤ .05 was considered to indicate the statistical significance for all tests. The ANOVA procedures were performed in SAS 9.2 (SAS Inc., USA), whereas Student's *t* and Friedman tests were performed in SPSS 22.0 (IBM Analytics, USA).

RESULTS

The ANOVA results, summarized in Table 1 and Table 2, broadly showed the significant effect of load on the facet joint motion, especially on the flexion (p = .003~.050, η^2 = .307~.526) and lateral bending (p = .001~.049, η^2 = .306~.593) and superior-inferior (p = .003~.050, η^2 = .290~.510) translation wherein a larger magnitude of the load caused consistently greater flexion and lateral bending and subsequently greater superior-inferior translation across all facet joints (Figure 5 and Figure 6). The averaged data across all four time instances and two facets on both sides revealed that lifting a load of 13.5 kg caused respectively, 22%, 11%, 17%, and 69% more flexion and 24%, 30%, 18%, and 7% more superior translation in L2-L3, L3-L4, L4-L5, and L5-S1 facet joints than lifting a load of 9 kg; 42%, 21%, 24%, and 590% more flexion and 15%, 28%, 19%, and 7% more superior translation than lifting a load of 4.5 kg. Similarly, we observed a consistent increasing trend of the load effect—a trend at a particular time instance is consistent if the magnitude of the facet joint motions increased with the heavier load—on the lateral bending for the right facet joints across all segments; the trends were however inconsistent for the left side of L4-L5 and L5-S1 facet joints (Table 1 and Figure 5). Nevertheless, partial η^2 results showed medium to large effect size (>.059) of the load effects on both flexion and lateral bending motions and superior-inferior translation at almost all bilateral facet joints.

The load effect was not dominant and displayed mixed results for the twisting motion (Table 1 and Figure 5). For example, the right side of L2-L3 at 2.0 s (p = .037, η^2 = .337) and the left side of L5-S1 at 1.0 s and 1.5 s (p = .007~.022, η^2 = .380~.464) showed statistically significant and consistent trends of load effect, whereas the left side of L3-L4 at 1.0 s and 1.5 s (p = .014~.001, η^2 = .415~.567), and the right side of L4-L5 at 1.0 s (p = .004, η^2 = .493) exhibited statistically significant but inconsistent trends of load effect (Table 1 and Figure 5). Consequently, the medial-lateral and anterior-posterior translations, which are primarily a product of twisting and lateral bending motions, were found to be far less than superior-inferior translation and showed mostly the inconsistent trends of load effect (Table 2 and Figure 6).

In general, a trend of increased motion was observed across all facet joints for a more flexed posture. Nonetheless, the ANOVA results revealed significant load effect (p = .001~.050, η^2 = .306~.593) across all segments at the trunk-flexion postures of about 40° (or 1s) and 20° (or 1.5 s), whereas only L4-L5 facet joints showed significant load effect (p = .043~.003, η^2 = .305~.526) at the trunk-flexion posture of 60° (or 0.5 s) (Figures 5 and 6). At the upright posture (0º or 2 s), the load effect was mostly inconsistent and statistically insignificant for the majority of the facet joints (Figures 5 and 6). The post hoc analysis also revealed that the significant differences in the facet joint motions

TABLE 1: ANOVA Results (*p*-value and partial η^2) of Rotational Kinematics Data

		Right				Left			
		L2L3	*L3L4*	*L4L5*	*L5S1*	*L2L3*	*L3L4*	*L4L5*	*L5S1*
Time					Flexion				
0.5 s	p =	.101	.179	**.003**	.239	.524	.199	**.043**	.619
	η^2=	.249	.193	.526	.164	.078	.183	.305	.058
1.0 s	p =	**.024**	**.019**	**.007**	.449	**.036**	**.027**	**.021**	.401
	η^2 =	.373	.391	.461	.095	.333	.348	.362	.076
1.5 s	p =	**.039**	**.048**	**.017**	**.028**	**.045**	.625	**.031**	.103
	η^2 =	.328	.296	.399	.36	.325	.057	.331	.247
2.0 s	p =	.148	.894	.858	.116	**.017**	.802	.872	**.050**
	η^2 =	.212	.014	.019	.236	.398	.027	.017	.307
					Lateral Bending				
0.5 s	p =	.574	.128	.073	.371	.491	.135	.083	.715
	η^2 =	.073	.226	.229	.117	.082	.221	.236	.026
1.0 s	p =	**.011**	**.040**	**.034**	**.032**	.152	**.001**	.104	.205
	η^2 =	.434	.308	.346	.342	.213	.593	.208	.148
1.5 s	p =	**.009**	.779	**.007**	**.040**	.569	**.002**	.075	.211
	η^2 =	.448	.031	.46	.332	.068	.54	.242	.177
2.0 s	p =	**.007**	**.049**	.911	.205	.333	.072	.506	.413
	η^2 =	.464	.306	.012	.18	.128	.243	.082	.051
					Twisting				
0.5 s	p =	.070	.342	.058	.946	.377	.855	.577	.115
	η^2 =	.283	.126	.299	.007	.115	.019	.066	.237
1.0 s	p =	.422	.244	**.004**	.592	.203	**.001**	.138	**.007**
	η^2 =	.102	.162	.493	.063	.18	.567	.219	.464
1.5 s	p =	.106	.303	.083	.937	.209	**.014**	.247	**.022**
	η^2 =	.244	.139	.268	.008	.178	.415	.161	.380
2.0 s	p =	**.037**	.343	.059	.575	.133	.131	.28	.156
	η^2 =	.337	.125	.297	.067	.223	.224	.147	.207

Note. A boldface *p*-value denotes a statistical significance ($p \leq .05$).

induced by the incremental (by 4.5 kg) external loads were primarily observed at the middle phase (at the flexed postures of about 40° and 20°) than the end range (at the flexed posture of about 60°) of the lifting motion, strongly indicating that, during dynamic lifting, the load effect depends not only on the lumbar flexion but also on the dynamic nature (i.e., how the acceleration changes) of the lifting motion.

Overall, the L5-S1 facet joints exhibited distinct kinematic patterns from the rest of the facet joints. For instance, L5-S1 facet joints evinced greater lateral bending and twisting than L2-L3, L3-L4, and L4-L5 facet joints, whereas it showed substantially smaller amount of flexion throughout all time instances (Figure 5). This could be due to the changes in facet orientation from L2 to S1 vertebral segments (Table 3). The transverse facet angle data revealed that both inferior and superior aspects of L5 and S1 facets were oriented approximately 48~59° away from the midsagittal plane of the vertebrae, in particular, superior facet of S1 is 3~5° more oriented toward coronal plane than the inferior facet of L5 (Table 3). In contrast, L2,

TABLE 2: ANOVA Results (*p*-value and partial η^2) of Translational Kinematics Data

		Right				Left			
		L2L3	*L3L4*	*L4L5*	*L5S1*	*L2L3*	*L3L4*	*L4L5*	*L5S1*
Time					Anterior-Posterior				
0.5 s	p =	.847	.120	.112	.914	.919	.322	.494	.797
	η^2 =	.021	.233	.240	.011	.010	.132	.084	.028
1.0 s	p =	.313	**.040**	**.002**	.264	.203	**.038**	**.034**	.470
	η^2 =	.135	.332	.548	.153	.181	.336	.345	.090
1.5 s	p =	.623	.349	**.026**	**.025**	.931	.145	**.022**	**.046**
	η^2 =	.057	.123	.365	.368	.009	.214	.380	.325
2.0 s	p =	.663	.715	.664	.690	.118	**.021**	.507	.536
	η^2 =	.05	.041	.050	.045	.235	.383	.081	.075
					Superior-Inferior				
0.5 s	p =	.224	**.047**	**.006**	.206	.262	**.018**	**.012**	.185
	η^2 =	.171	.318	.469	.179	.154	.396	.414	.190
1.0 s	p =	**.034**	**.008**	**.006**	.141	**.024**	**.005**	**.015**	.195
	η^2 =	.345	.450	.472	.217	.373	.491	.409	.185
1.5 s	p =	**.032**	**.036**	**.050**	**.003**	**.027**	**.047**	**.024**	**.019**
	η^2 =	.345	.339	.290	.510	.363	.318	.398	.427
2.0 s	p =	.178	.967	.846	**.022**	**.026**	.626	.931	.314
	η^2 =	.194	.004	.021	.379	.366	.057	.009	.135
					Medial-Lateral				
0.5 s	p =	.607	.453	.618	.581	.980	.857	.495	.735
	η^2 =	.060	.094	.058	.066	.003	.019	.084	.038
1.0 s	p =	.113	.810	.371	.262	.772	.635	**.017**	.522
	η^2 =	.238	.026	.117	.154	.032	.055	.400	.078
1.5 s	p =	.617	.577	.178	.413	.608	.832	.065	**.021**
	η^2 =	.059	.066	.194	.105	.060	.023	.290	.375
2.0 s	p =	.491	.258	.662	.861	.125	.908	.338	**.031**
	η^2 =	.085	.156	.050	.019	.229	.012	.127	.336

Note. A boldface *p*-value denotes a statistical significance ($p \leq .05$).

L3, and L4 facets were approximately 25~48° oriented away from the midsagittal plane (Table 3). Similarly, the coronal facet angle data also showed that the facet joints of L4-L5 and L5-S1 segments were more coronally oriented than the facet joints of L2-L3 and L3-L4 segments (Table 3). Moreover, the sagittal facet angle of the inferior facets was found to be more vertically oriented toward the frontal plane from L2 to S1 segments, whereas the superior facets dramatically increased toward the posterior direction, thus creating a mismatch in orientation between two adjacent articulating facets, which was substantially high (17~19°) at the L5-S1 facet joint (Table 3).

The results revealed some significant left-right distinctions in the facet joint motions (Table 4). For example, the magnitudes of flexion of the left facet joints of L2-L3 and L3-L4 segments were significantly smaller than that of their right counterparts (Figure 5, Table 4). On the other hand, the lateral-medial translations of the left facet joints of L2-L3, L3-L4, and L4-L5 segments were significantly larger than that of their right counterparts throughout all time

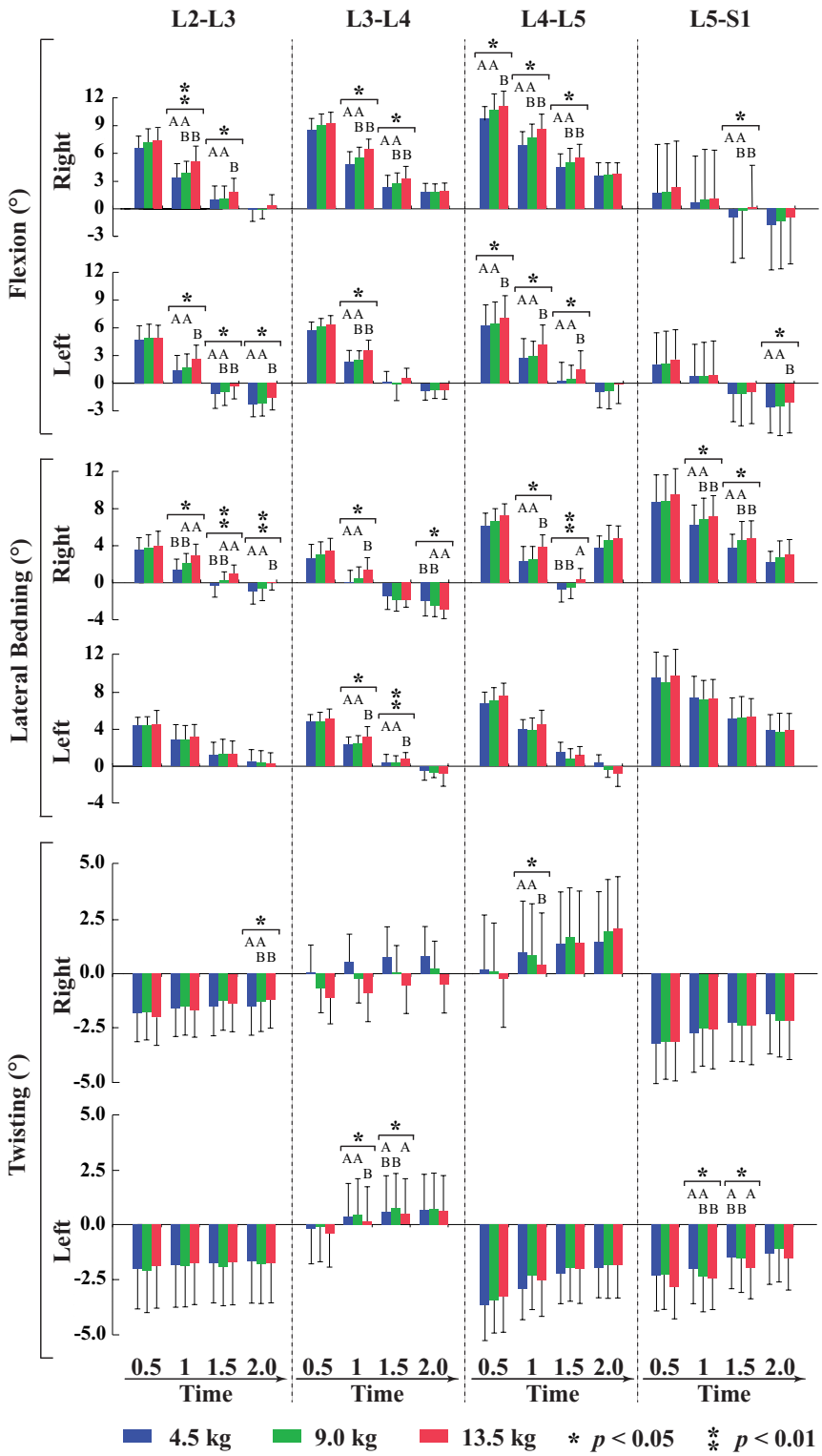

Figure 5. The mean and standard error of the facet joint rotational kinematics at different load levels and time instances. Asterisk indicates statistical significance of the load effect. Symbols A, B, and C denote the post hoc results within each time instance wherein group means with the same letters were not significantly different, but with different letters were significantly different.

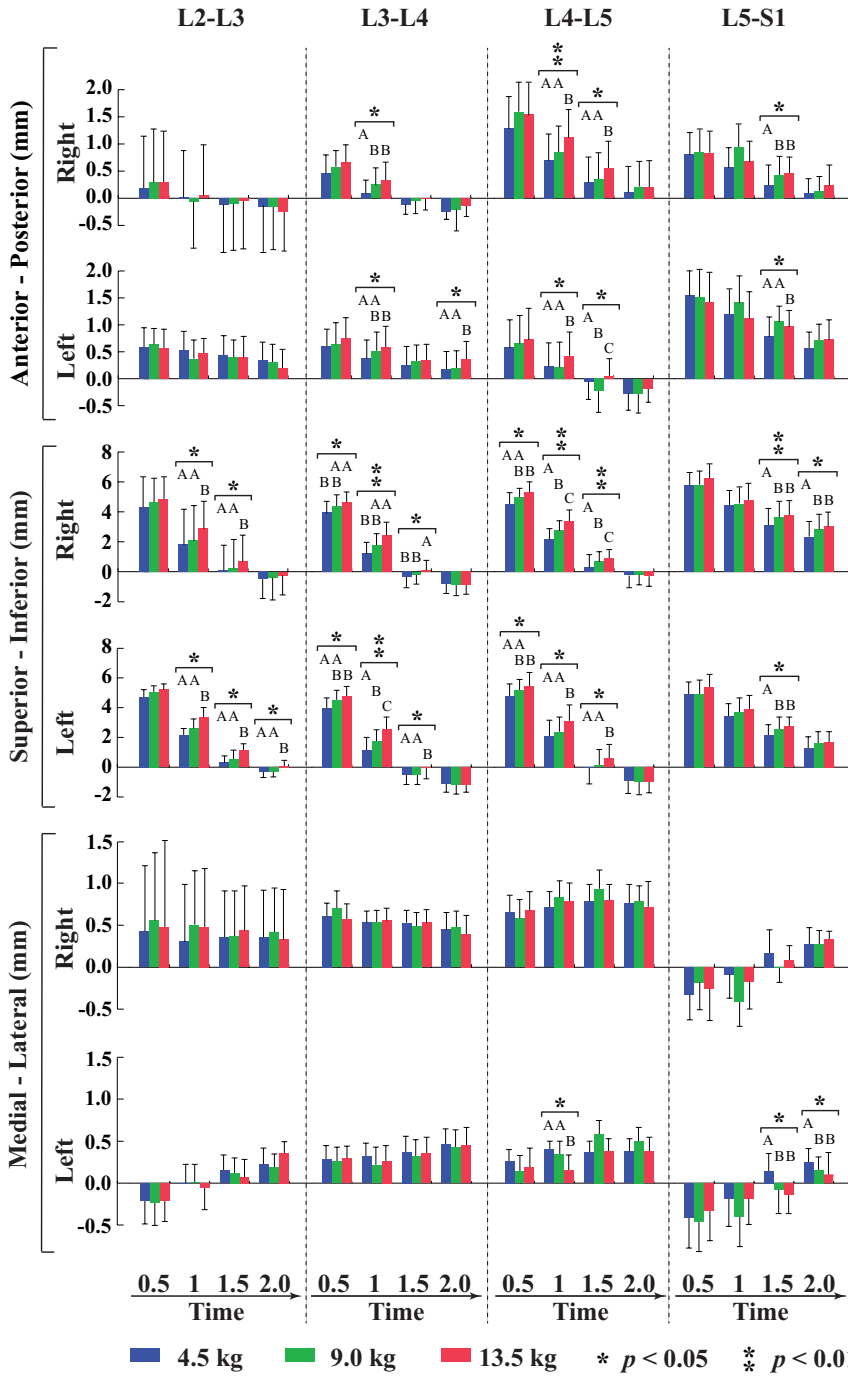

Figure 6. The mean and standard error of the facet joint translational kinematics at different load levels and time instances. Asterisk indicates statistical significance of the load effect. Symbols A, B, and C denote the post hoc results within each time instance wherein group means with the same letters were not significantly different, but with different letters were significantly different.

TABLE 3: Mean ± Standard Deviation Data (n = 11) of Transverse Facet Angle (α), Sagittal Facet Angle (β), and Coronal Facet Angle (γ) Measurements

	Superior			Inferior		
	Right	Left	*p*-value	Right	Left	*p*-value
			Transverse facet angle			
L2	26.0 ± 10.9	25.9 ± 10.6	.917	27.5 ± 12.8	26.2 ± 8.9	.549
L3	28.8 ± 13.1	31.0 ± 16.0	.367	33.6 ± 15.7	39.1 ± 15.9	**.046**
L4	33.5 ± 16.4	38.4 ± 14.3	**.041**	48.6 ± 13.6	47.4 ± 13.2	.511
L5	48.3 ± 14.2	50.2 ± 15.2	.275	55.9 ± 6.8	51.4 ± 6.4	**.050**
S1	58.9 ± 11.1	56.1 ± 8.8	.207			
			Sagittal facet angle			
L2	82.8 ± 2.0	83.2 ± 3.7	.595	81.7 ± 4.2	83.7 ± 4.5	**.044**
L3	86.1 ± 4.3	87.6 ± 4.4	.120	82.2 ± 4.9	82.8 ± 3.8	.475
L4	91.7 ± 5.9	90.3 ± 4.7	.153	85.0 ± 5.1	84.2 ± 2.1	.522
L5	98.0 ± 6.7	97.7 ± 5.1	.806	88.7 ± 9.8	91.3 ± 5.1	.374
S1	107.9 ± 6.7	108.6 ± 8.0	.519			
			Coronal facet angle			
L2	90.7 ± 3.2	88.6 ± 4.0	.117	89.3 ± 4.4	87.8 ± 2.8	.263
L3	87.7 ± 4.7	90.2 ± 4.3	**.040**	88.7 ± 5.1	86.3 ± 2.9	.874
L4	83.5 ± 5.1	87.6 ± 2.8	**.012**	85.0 ± 3.2	83.4 ± 5.0	**.018**
L5	83.4 ± 7.2	83.8 ± 3.6	.882	82.4 ± 9.2	82.4 ± 4.2	.374
S1	83.2 ± 4.2	86.7 ± 4.4	**.043**			

Note. All angles are in degrees (°).

instances (Table 4, Figure 6). Similarly, the magnitudes of the lateral bending and twisting of the left facet joints—in particular, at L5-S1 segment—were observed to be significantly larger than their right counterparts across all time instances (Table 4, Figure 5). Other segment-wise distinctions were also observed—such as the twisting of L4-L5 facet joints and the anterior-posterior and medial-lateral translations of all facet joints (Table 4, Figure 6)—which could be due to the facet tropism—a left-right difference in facet orientation.

The facet tropism was prevalent at all levels, with more significant differences ($p < .05$) in the facet orientations at L3 and L4 levels (Table 3). The transverse facet angle data showed significantly higher coronal orientation (~5°) in the articulating facets (inferior and superior aspects of L3 and L4, respectively) of the left L3-L4 facet joint compared with its right counterpart (Table 3). In contrast, coronal facet angle data indicated a more lateral orientation for the superior aspect of L4 (~4.5°) facet of the right L3-L4 facet joint compared with its left counterpart. The articulating facets (inferior and superior aspects of L5 and S1, respectively) of the left L5-S1 facet joint showed significantly more sagittal orientation (L5: ~4.5° and S1: 3.5°) than their right counterparts (Table 3). Other noteworthy findings were that the left aspects of all facet joints were more laterally oriented than their right counterparts; and the articulating facets of the left L2-L3 facet joint and right L4-L5 facet joint were, respectively, more posteriorly and medially oriented than their right counterparts (Table 3).

DISCUSSION

In this study, a DSX system, with the acuity to discern the facet joint kinematics, imaged the participants' lumbar motion while dynamic lifting was performed. Overall, the results showed significant load effects on the facet joint kinematics at different trunk-flexion positions (or time instances) wherein a heavier load mostly

TABLE 4: Student's T Test Results to Indicate the Left-Right Differences in Rotational and Translational Kinematics of the Facet Joints

Time	Anterior-Posterior	Superior-Inferior	Medial-Lateral	Flexion	Lateral Bending	Twisting
			L2-L3			
0.5 s	.194	.287	**.001**	**.038**	**<.000**	**.001**
1.0 s	.100	.343	**.009**	**.030**	**.002**	**.002**
1.5 s	**.050**	.382	**.025**	**.041**	.312	**.004**
2.0 s	**.040**	.503	**.050**	**.048**	.656	**.004**
			L3-L4			
0.5 s	.632	.843	**.019**	**<.000**	**<.000**	.269
1.0 s	.211	.98	**.027**	**<.000**	**.002**	.734
1.5 s	**.037**	.753	**.043**	**<.000**	.162	.886
2.0 s	**.029**	.549	.966	**<.000**	**<.000**	.783
			L4-L5			
0.5 s	**.014**	.772	**.002**	.533	**<.000**	.177
1.0 s	**.031**	.736	**<.000**	.474	**<.000**	.781
1.5 s	.107	.557	**.006**	.376	**.041**	.880
2.0 s	.207	.353	**.019**	.408	**.006**	.687
			L5-S1			
0.5 s	.463	.190	.463	.437	**<.000**	**<.000**
1.0 s	.864	.238	.864	.42	**<.000**	**<.000**
1.5 s	.501	.105	.501	.237	**<.000**	**.002**
2.0 s	.376	.097	.376	.199	**<.000**	**.005**

Note. A boldface *p*-value denotes a statistical significance ($p \leq .05$).

caused increased facet joint motions. Such increases revealed the contribution of facet joints, in varying degrees, to resist the additional shear force produced along the spine in order to prevent excessive rotation and translation of the intervertebral disc (Adams & Hutton, 1981). The load effect was more pronounced on the flexion motion as compared with twisting and lateral bending of the facet joints, reflecting the fact that participants performed a two-handed sagittally symmetric lifting task that bore minimal amount of twisting and lateral bending of the spine. Nevertheless, higher magnitudes of lateral bending were observed owing to anterolateral and posterolateral orientations of the inferior and superior aspects of the facet joints, respectively.

In general, we observed greater facet joint motions in a more flexed trunk posture. It is not a surprise considering that as the trunk flexed more, both the center of masses of the upper body and the external load moved more away from the base of the spine, and consequently imposed an increasing amount of bending moment and anterior shear forces in the spine. Interestingly, the load effect was more salient in the middle phase (20°~40°) than the end range (~ 60° or 0°) of the lifting task, indicating a complex, dynamic interplay between the load and trunk movements in modulating the load effect. As the acceleration of the load reached its peak during the middle phase, it appears the load effect was more dependent on the dynamic nature of the load (i.e., its acceleration profile) than the trunk flexion. In this study, the differences in the magnitudes of facet joint motions between different postures were more notable than the differences due to load effect within the postures. This may be due to the reason that we discretized the lumbar flexion-extension at every 20°, and

therefore the increased mechanical instability by a flexed- and loaded-spine was biomechanically more substantial than simply by increasing the load by 4.5 kg at those postures. Nevertheless, a much higher load or greater increments may produce a different result.

The L5-S1 facet joints exhibited distinct motions from the remaining facet joints, which could be due to their unique articular joint structure. The opposing articular facet surfaces of L2, L3, and L4 segments were observed to be more vertically and sagittaly oriented, consequently restraining each other during twisting and lateral bending motions, whereas allowing greater motion to occur along the sagittal plane. On the contrary, the superior facets of S1 segment were observed to be more aligned with the frontal plane than the facets of other segments (L2~L5). As a result, there is more space or laxity (~5°) at the L5-S1 articulating joint to permit more motion in the medial-lateral direction than the remaining joints. Previous studies examining lumbar facet orientation reported similar findings (Kozanek et al., 2009; Masharawi et al., 2004; Noren et al., 1991; Panjabi et al., 1993). Furthermore, the sagital facet angle data implied a higher mismatch in the the vertical orientation of L5-S1 facet joint since the superior facet of S1 segment was about 17° to 19° more posteriorly oriented than the inferior facet of L5, thus providing more mobility in twisting and lateral bending. Due to such large amount of posterior inclination of the facets of S1 segment, the superior-inferior translations of L5-S1 facet joints were substantially greater than the remaining facet joints.

In this study, facet tropism—an asymmetry of the facet joint orientation between left and right sides—was observed across all segments. Such right-left differences in orientation influenced their motion (both in magnitude and direction) since eccentric forces were exerted on these asymmetric facet joints during the extension movement of the loaded- and flexed-spine. For this study, if we define facet tropism as a bialteral angle difference $>3°$, then facet tropism was significantly observed at the articulating facets of L3-L4 and L5-S1 facet joints as in a previous study (Zhou, Teng, Zhang, Lei, & Jiang, 2018). It is noteworthy that there was some evidence emerging from previous studies to suggest facet tropism inducing facet-centered pain and leading to disc degeneration, facet degenerative spondylolisthesis, and other degenerative conditions (Alonso et al., 2017; Grogan et al., 1997; Murtagh, Paulsen, & Rechtine, 1991). This study presents a hitherto baseline dataset of facet orientation and tropism for a healthy participant group, and how left-right distinct coupling patterns influenced facet joint kinematics during sagittally symmetric lifting. Future studies should explore further the influence of facet tropism on the spinal stability during different functional activities to comprehend the etiology of the facet-related low back pain.

In general, the facet joints are weak in tensile strength. For example, a previous study based on finite element models showed that the load to tensile and compressive failures of facet capsular ligament were about 600-750N and 6000N, respectively (Yang & King, 1984). During a load-lifting task, the likelihood of tensile failure of facet capsular ligament is greater at a trunk-flexion position since a flexed posture imposes a higher bending moment (i.e., tensile force) on the facet joints compared with an upright trunk posture. Therefore, although the changes in facet joint motions are of relatively small magnitude, even nominal deviations from the normal range of facet joint motions could increase the risk of impingement between the adjacent facet surfaces and inflict significant pain and potentially lead to lumbar joint instability.

A few limitations of this study are recognized. First, due to the limited field of view of the DSX system, portions of the lumbar spine (L1 vertebrae) and initial (~75º flexion) posture could not be imaged, which consequently prevented measuring the initial position as well as L1-L2 facet joints. Second, the trunk-flexion positions at each time instance varied slightly across the participants, even though the pace of the trials (or the body movement) was carefully controlled using a metronome. Third, data of both male and female participants were combined in the current analysis, with some justification from a previous study showing no gender disparity in facet orientation across the

thoracolumbar spine (Masharawi et al., 2004). Fourth, a small sample size might contribute to some statistical nonsignificance. An ideal study would include a greater number of participants to allow explicit assessment of the gender difference with greater confidence.

In conclusion, the present study, believed to be one of the earliest in vivo investigations of the lumbar facet joint biomechanics, has identified and quantified important dynamic, load-dependent changes in facet joints of a flexed- and loaded-spine in relation to the facet orientation. With clearer and quantitative knowledge of facet joint kinematics for the lumbar spine, we can better understand how various occupational activities may mechanically induce LBP differently, thereby providing the scientific basis for the design of safer and healthier workplaces.

ACKNOWLEDGMENTS

This work was funded by a research grant (R21OH00996) from the Centers for Disease Control and Prevention/National Institute for Occupational Safety and Health.

KEY POINTS

- A larger magnitude of the external load caused greater flexion and lateral bending, and subsequently greater superior-inferior translations across all facet joints.
- The effects of load were more salient at the middle phase than the end range of a dynamic lifting task.
- L2-L3, L3-L4, and L4-L5 facet joints showed greater flexion motion and medial-lateral translation than L5-S1 facet joints, whereas L5-S1 facet joints showed comparatively larger lateral bending and twisting motions and superior-inferior translations than the remaining joints.
- The articulating facets at the L5-S1 joint are substantially more coronally and posteriorly oriented than the facets at the L2-L3, L3-L4, and L4-L5 joints.
- Left-right asymmetry in orientation was observed across all facet joints, in particular, at the articulating facets of L3-L4 and L5-S1 joints.

REFERENCES

Adams, M., & Hutton, W. (1981). The relevance of torsion to the mechanical derangement of the lumbar spine. *Spine (Phila Pa 1976)*, *6*(3), 241–248.

Aiyangar, A. K., Zheng, L., Anderst, W., & Zhang, X. (2015). Apportionment of lumbar L2–S1 rotation across individual motion segments during a dynamic lifting task. *Journal of Biomechanics*, *48*(13), 3709–3715.

Aiyangar, A. K., Zheng, L., Tashman, S., Anderst, W. J., & Zhang, X. (2014). Capturing three-dimensional in vivo lumbar intervertebral joint kinematics using dynamic stereo-X-ray imaging. *Journal of Biomechanical Engineering*, *136*(1). doi:10.1115/1.4025793

Alonso, F., Kirkpatrick, C. M., Jeong, W., Fisahn, C., Usman, S., Rustagi, T., . . . Tubbs, R. S. (2017). Lumbar facet tropism: A comprehensive review. *World Neurosurgery*, *102*(Supplement C), 91–96. doi:https://doi.org/10.1016/j.wneu.2017.02.114

Bigos, S. J., Spengler, D. M., Martin, N. A., Zeh, J., Fisher, L., Nachemson, A., & Wang, M. H. (1986). Back injuries in industry: A retrospective study. II. Injury factors. *Spine (Phila Pa 1976)*, *11*(3), 246–251.

BLS. (2016). Nonfatal occupational injuries and illnesses requiring days away from work, 2015. Retrieved from https://www.bls.gov/news.release/pdf/osh2.pdf

Cohen, J. (1988). *Statistical power analysis for the behavioral sciences*. Hillsdale, NJ: Erlbam.

Crawford, N. R., Duggal, N., Chamberlain, R. H., Park, S. C., Sonntag, V. K., & Dickman, C. A. (2002). Unilateral cervical facet dislocation: Injury mechanism and biomechanical consequences. *Spine (Phila Pa 1976)*, *27*(17), 1858–1864; discussion 1864.

DePalma, M. J., Ketchum, J. M., & Saullo, T. (2011). What is the source of chronic low back pain and does age play a role? *Pain Medicine*, *12*(2), 224–233. doi:10.1111/j.1526-4637.2010.01045.x

Granata, K., & Marras, W. (1993). An EMG-assisted model of loads on the lumbar spine during asymmetric trunk extensions. *Journal of Biomechanics*, *26*(12), 1429–1438.

Grobler, L. J., Robertson, P. A., Novotny, J. E., & Pope, M. H. (1993). Etiology of spondylolisthesis: Assessment of the role played by lumbar facet joint morphology. *Spine (Phila Pa 1976)*, *18*(1), 80–91.

Grogan, J., Nowicki, B. H., Schmidt, T. A., & Haughton, V. M. (1997). Lumbar facet joint tropism does not accelerate degeneration of the facet joints. *American Journal of Neuroradiology*, *18*(7), 1325–1329.

Hoogendoorn, W. E., Bongers, P. M., de Vet, H. C., Douwes, M., Koes, B. W., Miedema, M. C., . . . Bouter, L. M. (2000). Flexion and rotation of the trunk and lifting at work are risk factors for low back pain: Results of a prospective cohort study. *Spine (Phila Pa 1976)*, *25*(23), 3087–3092.

Hoogendoorn, W. E., van Poppel, M. N., Bongers, P. M., Koes, B. W., & Bouter, L. M. (1999). Physical load during work and leisure time as risk factors for back pain. *Scandinavian Journal of Work, Environment & Health*, *25*(5), 387–403.

Igarashi, A., Kikuchi, S., Konno, S., & Olmarker, K. (2004). Inflammatory cytokines released from the facet joint tissue in degenerative lumbar spinal disorders. *Spine (Phila Pa 1976)*, *29*(19), 2091–2095.

Katz, J. N. (2006). Lumbar disc disorders and low-back pain: Socioeconomic factors and consequences. *Journal of Bone and Joint Surgery, 88 Suppl 2*, 21–24. doi:10.2106/JBJS.E.01273

Kozanek, M., Wang, S., Passias, P. G., Xia, Q., Li, G., Bono, C. M., . . . Li, G. (2009). Range of motion and orientation of the lumbar facet joints in vivo. *Spine (Phila Pa 1976)*, *34*(19), E689–696. doi:10.1097/BRS.0b013e3181ab4456

Lee, J. B. E., & Anderst, W. J. (2010). *Lumbar spine motion during functional movement: In vivo validation of flexion/extension*

movement tracking. Paper presented at the 3rd Annual Lumbar Spine Research Society Meeting, Chicago, IL.

Liu, X., Huang, Z., Zhou, R., Zhu, Q., Ji, W., Long, Y., & Wang, J. (2017). The effects of orientation of lumbar facet joints on the facet joint contact forces: An in vitro biomechanical study. *Spine (Phila Pa 1976)*, *43*(4): E216–E220.

Manchikanti, L., Singh, V., Pampati, V., Damron, K. S., Barnhill, R. C., Beyer, C., & Cash, K. A. (2001). Evaluation of the relative contributions of various structures in chronic low back pain. *Pain Physician*, *4*(4), 308–316.

Marras, W. S., Ferguson, S. A., Burr, D., Davis, K. G., & Gupta, P. (2004). Spine loading in patients with low back pain during asymmetric lifting exertions. *The Spine Journal*, *4*(1), 64–75.

Marras, W. S., Lavender, S. A., Leurgans, S. E., Fathallah, F. A., Ferguson, S. A., Gary Allread, W., & Rajulu, S. l. (1995). Biomechanical risk factors for occupationally related low back disorders. *Ergonomics*, *38*(2), 377–410.

Marras, W. S., & Sommerich, C. M. (1991). A three-dimensional motion model of loads on the lumbar spine: I. Model structure. *Human Factors*, *33*(2), 123–137.

Masharawi, Y., Rothschild, B., Dar, G., Peleg, S., Robinson, D., Been, E., & Hershkovitz, I. (2004). Facet orientation in the thoracolumbar spine: Three-dimensional anatomic and biomechanical analysis. *Spine (Phila Pa 1976)*, *29*(16), 1755–1763.

Masharawi, Y., Rothschild, B., Salame, K., Dar, G., Peleg, S., & Hershkovitz, I. (2005). Facet tropism and interfacet shape in the thoracolumbar vertebrae: Characterization and biomechanical interpretation. *Spine (Phila Pa 1976)*, *30*(11), E281–E292.

McGill, S., & Norman, R. (1986). 1986 Volvo award in biomechanics: Partitioning of the L4-L5 dynamic moment into disc, ligamentous, and muscular components during lifting. *Spine (Phila Pa 1976)*, *11*(7), 666–678.

Murtagh, F., Paulsen, R., & Rechtine, G. (1991). The role and incidence of facet tropism in lumbar spine degenerative disc disease. *Journal of Spinal Disorders*, *4*(1), 86–89.

Naserkhaki, S., Jaremko, J. L., Adeeb, S., & El-Rich, M. (2016). On the load-sharing along the ligamentous lumbosacral spine in flexed and extended postures: Finite element study. *Journal of biomechanics*, *49*(6), 974–982.

Noren, R., Trafimow, J., Andersson, G., & Huckman, M. (1991). The role of facet joint tropism and facet angle in disc degeneration. *Spine (Phila Pa 1976)*, *16*(5), 530–532.

Otsuka, Y., An, H. S., Ochia, R. S., Andersson, G. B., Orías, A. A. E., & Inoue, N. (2010). In vivo measurement of lumbar facet joint area in asymptomatic and chronic low back pain subjects. *Spine (Phila Pa 1976)*, *35*(8), 924.

Panjabi, M. M., Oxland, T., Takata, K., Goel, V., Duranceau, J., & Krag, M. (1993). Articular facets of the human spine quantitative three-dimensional anatomy. *Spine (Phila Pa 1976)*, *18*(10), 1298–1310.

Popovich, J. M., Welcher, J. B., Hedman, T. P., Tawackoli, W., Anand, N., Chen, T. C., & Kulig, K. (2013). Lumbar facet joint and intervertebral disc loading during simulated pelvic obliquity. *The Spine Journal*, *13*(11), 1581–1589.

Sharma, M., Langrana, N. A., & Rodriguez, J. (1995). Role of ligaments and facets in lumbar spinal stability. *Spine (Phila Pa 1976)*, *20*(8), 887–900.

Vaccaro, A. R., Falatyn, S. P., Flanders, A. E., Balderston, R. A., Northrup, B. E., & Cotler, J. M. (1999). Magnetic resonance evaluation of the intervertebral disc, spinal ligaments, and spinal cord before and after closed traction reduction of cervical spine dislocations. *Spine (Phila Pa 1976)*, *24*(12), 1210–1217.

Yang, K. H., & King, A. (1984). Mechanism of facet load transmission as a hypothesis for low-back pain. *Spine (Phila Pa 1976)*, *9*(6), 557–565.

Zhang, X., Xiong, J., & Bishop, A. M. (2003). Effects of load and speed on lumbar vertebral kinematics during lifting motions. *Human Factors*, *45*(2), 296–306.

Zhou, Q., Teng, D., Zhang, T., Lei, X., & Jiang, W. (2018). Association of facet tropism and orientation with lumbar disc herniation in young patients. *Neurological Sciences*, 1–6.

Suman K. Chowdhury is an assistant research scientist in the Department of Industrial and Systems Engineering at the Texas A&M University, College Station, TX. He obtained his PhD in Industrial Engineering from the West Virginia University in 2016.

Ryan M. Byrne is a PhD student in the Department of Mechanical Engineering and Materials Science at the University of Pittsburgh, Pittsburgh, PA.

Yu Zhou is a PhD student in the Department of Industrial & Systems Engineering at the Texas A&M University, College Station, TX. He received his MS in Mechanical Engineering from the University of Pittsburgh in 2017.

Xudong Zhang is a professor in the Department of Industrial & Systems Engineering at the Texas A&M University, College Station, TX. He received his PhD in Industrial and Operations Engineering from the University of Michigan in 1997.

Date received: December 20, 2017
Date accepted: June 22, 2018